ANL-77-56

ADVANCED FUEL CELL DEVELOPMENT

Progress Report for
April–June 1977

by

J. P. Ackerman, K. Kinoshita, J. W. Sim,
R. Swaroop, and P. A. Nelson

U of C-AUA-USERDA

ARGONNE NATIONAL LABORATORY, ARGONNE, ILLINOIS

Prepared for the U. S. ENERGY RESEARCH
AND DEVELOPMENT ADMINISTRATION
under Contract W-31-109-Eng-38

Printed in the United States of America
Available from
National Technical Information Service
U. S. Department of Commerce
5285 Port Royal Road
Springfield, Virginia 22161
Price: Printed Copy $4.00; Microfiche $3.00

Distribution Category:
Energy Conversion
(UC-93)

ANL-77-56

ARGONNE NATIONAL LABORATORY
9700 South Cass Avenue
Argonne, Illinois 60439

ADVANCED FUEL CELL DEVELOPMENT

Progress Report for
April—June 1977

by

J. P. Ackerman, K. Kinoshita, J. W. Sim,
R. Swaroop, and P. A. Nelson

Chemical Engineering Division

August 1977

TABLE OF CONTENTS

	Page
ABSTRACT	1
SUMMARY	1
I. INTRODUCTION	2
II. ELECTROLYTE DEVELOPMENT	3
A. Preparation and Characterization of Electrolytes	3
B. Phase and Structural Stability of $LiAlO_2$	5
III. CELL TESTING	5
A. Wet-Seal Protection	6
B. Cell Operation	6
IV. COMPONENT ANALYSIS AND DEVELOPMENT	9
A. Post-Test Observations	9
B. Characterization of Porous Nickel Electrodes	9
C. Tile Diagnostics	13
REFERENCES	16

LIST OF FIGURES

No.	Title	Page
1.	Thermograms of Electrolyte Powders	4
2.	Schematic of CS-Series Cells	7
3.	Comparison of Cell Performance of CS-Series Cells	7
4.	Mercury Penetration of Nickel Electrodes	11
5.	Distribution of Pores in Nickel Electrodes	12
6.	Modified Static Creep Apparatus	13
7.	Thermal Expansion and Creep-Rate Measurements on Electrolyte Tiles	15

LIST OF TABLES

No.	Title	Page
1.	Structural and Performance Characteristics of CS-Series Cells	8
2.	Porosities and Surface Areas of Porous Nickel Electrodes	11
3.	Thermal Measurements on Electrolyte Tiles	14

CHEMICAL ENGINEERING DIVISION

ADVANCED FUEL CELL DEVELOPMENT

April—June 1977

by

J. P. Ackerman, K. Kinoshita, J. W. Sim
R. Swaroop, and P. A. Nelson

ABSTRACT

This report describes advanced fuel cell research and development activities at Argonne National Laboratory (ANL) during the period April—June 1977. These efforts have been directed toward understanding and improvement of molten-carbonate-electrolyte fuel cells operating at temperatures near 923 K.

A primary focus of the work has been on developing electrolyte structures which have high strength and conductivity, as well as good electrolyte retention, and on developing methods of synthesis for electrolyte structures that are amenable to mass production. A low temperature synthesis which produces material having rodlike particles of β-$LiAlO_2$ has been refined and is now used for preparing electrolytes.

Cell testing is essential for understanding and evaluating individual component behavior and the interactions of the components under realistic operating conditions. Most of the testing to date has been conducted in a 7-cm (2 3/4-in.)-dia cylindrical cell with Type 316 stainless steel housings and current collectors, a nickel anode, and a nickel oxide cathode. Testing has begun to probe the roles of anode, cathode, and electrolyte in cell performance, and has provided verification of an acceptable technique for prevention of seal corrosion for at least 1400 hours.

Components evaluation and development include post-test analysis and evaluation of cell components and materials, as well as development of out-of-cell diagnostic tests for the individual components. Particular attention is being paid to evaluation of the physical properties of the electrolyte and of the porous nickel and nickel oxide electrodes.

SUMMARY

Electrolyte Development

Preparation and Characterization of $LiAlO_2$. A new synthesis of $LiAlO_2$ repeatedly and uniformly yields rods of β-$LiAlO_2$ having aspect ratios of 3 to 6. Some control of particle size may be possible. Special precautions to ensure completion of the carbonation reaction of the hydroxides and removal of all product water are necessary to provide a suitable powder for pressing

electrolyte structures (tiles). Differential thermal analysis is being used to follow carbonation and water removal.

Phase and Structural Stability of $LiAlO_2$. Rods of β-$LiAlO_2$, previously shown to transform to square bipyramidal particles of γ-$LiAlO_2$ at 973 K in 100 h, appear to be completely unchanged in a variety of gaseous atmospheres at 923 K for periods of nearly 1000 h.

Cell Testing

Wet Seal Protection. An aluminizing process providing excellent wet seal corrosion protection for at least 1400 h is described. It is a simple process--flame spraying followed by a single heat-treatment step--that appears to be well suited to mass production.

Cell Operation. Experience with Cells CS-1 through CS-4 suggests that matching of pore size distribution and electrolyte content is essential for good cell performance. Optimization of the size distribution of $LiAlO_2$ particles in the electrolyte is under way.

Component Analysis and Development

Post Test Analysis. The cathode sides of electrolyte tiles continue to show diffused NiO layers. Protected wet seals are corrosion-free after 1400 h of operation.

Characterization of Porous Electrodes. Theoretical considerations and initial measurements of electrode porosity, pore size distribution, and surface area are presented and related to cell performance.

Characterization of Electrolyte Tiles. The static creep apparatus has been modified and measurements have been made of the thermal expansion and creep behavior of several tile samples.

I. INTRODUCTION

The advanced fuel cell studies at Argonne National Laboratory (ANL) are part of the ERDA Second Generation Fuel Cell Program. This ERDA program has as its goal the earliest possible introduction of coal-fueled, high-efficiency electric generators based on molten carbonate fuel cells, and is being carried out primarily by industrial contractors. At the present stage of development, the primary thrust of the program is directed toward development of the fuel cell itself.

Molten carbonate fuel cells consist of a porous nickel alloy anode, a porous nickel oxide cathode, an electrolyte structure separating the anode and cathode, and appropriate metal cell housings or, in the case of stacks of cells, cell separator plates. The cell housings (or separator plates) bear upon the electrolyte structure to form a seal between the environment and the anode and cathode gas compartments. The electrolyte structure, which is commonly called a "tile," is a composite structure of solid $LiAlO_2$ particles and a mixture of alkali metal carbonates which are liquid at the cell operating temperature of 923 K. At the anode, hydrogen and carbon monoxide in the fuel gas react with

carbonate ion from the electrolyte to form carbon dioxide and water, giving up electrons to the external circuit. At the cathode, carbon dioxide and oxygen react and accept electrons from the external circuit to re-form carbonate ion, which is conducted through the electrolyte to the anode. In a practical cell stack, CO_2 for the cathode would be obtained from the anode exhaust.

The ANL contribution to the program is intended to provide understanding of cell behavior and improved components and processes. More improvements are needed in the electrolyte tile than in any other single component. For this reason, electrolyte development is receiving special attention at ANL. Characterization of tile properties and the relation of its properties to tile behavior in cells is of major importance. Determination of stability of tile materials is also of high priority.

Operation of cells is required for assessment of the behavior of tiles and other components and for understanding of the performance and life-limiting mechanisms at work within the cell. Cell operation is, of course, coupled with a diagnositc effort and a materials-development effort, with the aim of developing cells of adequate performance and longevity for realistic component testing.

II. ELECTROLYTE DEVELOPMENT

A. Preparation and Characterization of Electrolytes

A method has been devised for preparing electrolyte mixtures of Li_2CO_3-K_2CO_3 containing rod-shaped particles of beta lithium aluminate (β-$LiAlO_2$) by the reactions among γ-Al_2O_3, LiOH-KOH, and CO_2. Initial work on this method was described in the preceding quarterly report (ANL-77-29). The rodlike particles are intended to lend strength to electrolyte structures without adverse effects on conductivity. During this reporting period, investigations of the synthesis of the rodlike β-$LiAlO_2$ particles have been continued. The method is not particularly sensitive to changes in reaction temperature or other synthesis parameters; it routinely yields rods with submicrometer diameters and aspect (length/diameter) ratios of three to six. Preliminary experiments have indicated that, by varying the reaction temperature, the diameter of the rods can be varied from approximately 0.5 to 1 μm without changing the aspect ratio; however, this temperature effect has not yet been investigated thoroughly. Instead, present work has centered on establishing conditions for complete conversion of the alkali hydroxides to carbonates.

Briefly, the synthesis is carried out by first slurrying finely divided γ-Al_2O_3 (Degussa type "C") in a concentrated aqueous solution containing sufficient LiOH for reaction with the Al_2O_3 to form $LiAlO_2$, as well as a sufficient excess of LiOH and KOH to form a usable electrolyte structure or "tile" upon reaction with CO_2. The slurry is evaporated to dryness and treated with CO_2. Reaction of CO_2 and alkali hydroxides to form carbonates is very exothermic (-96 kJ/mol for Li_2CO_3 and -150 kJ/mol for K_2CO_3)[1]; the heat released is sufficient to cause Al_2O_3 and LiOH to react, forming the rodlike β-$LiAlO_2$. In principle, all the hydroxides should be readily converted to carbonate, and the mixture should be ready for pressing to form a tile. In practice, however, sometimes conversion is incomplete and/or water of reaction remains in the mixture. Investigations of the parameters governing the production of satisfactory tile material are in progress.

A differential thermal analyzer (DuPont Model 900) is used to monitor the progress of the carbonation reaction between CO_2 and LiOH-KOH. When the reaction has gone to completion and all product water has been removed, a thermogram shows a single endotherm at ∿763 K (Fig. 1, Curve B). If product water has not been completely removed or if reaction is not complete, other endotherms are seen at lower temperatures. The endotherm at 643 K (Fig. 1, Curve A) is typical of incomplete carbonation, or retained product water.

The usual carbonation procedure has been to pass CO_2 over the dried, powdered mixture of LiOH, KOH, and Al_2O_3 without heating, but this has not always given complete conversion. Moreover, CO_2 or CO_2/inert gas mixtures flowing upward through the powdered mixture in a vertical glass tube have caused agglomeration of the powder and formation of a shell of carbonate on the agglomerated particles, which impedes the reaction. Since the carbonation reaction is so highly favored, an efficient, one-step method can probably be devised for carrying out the reaction on an industrial scale; however, the following procedure, which produces suitable material, is used in laboratory-scale preparations.

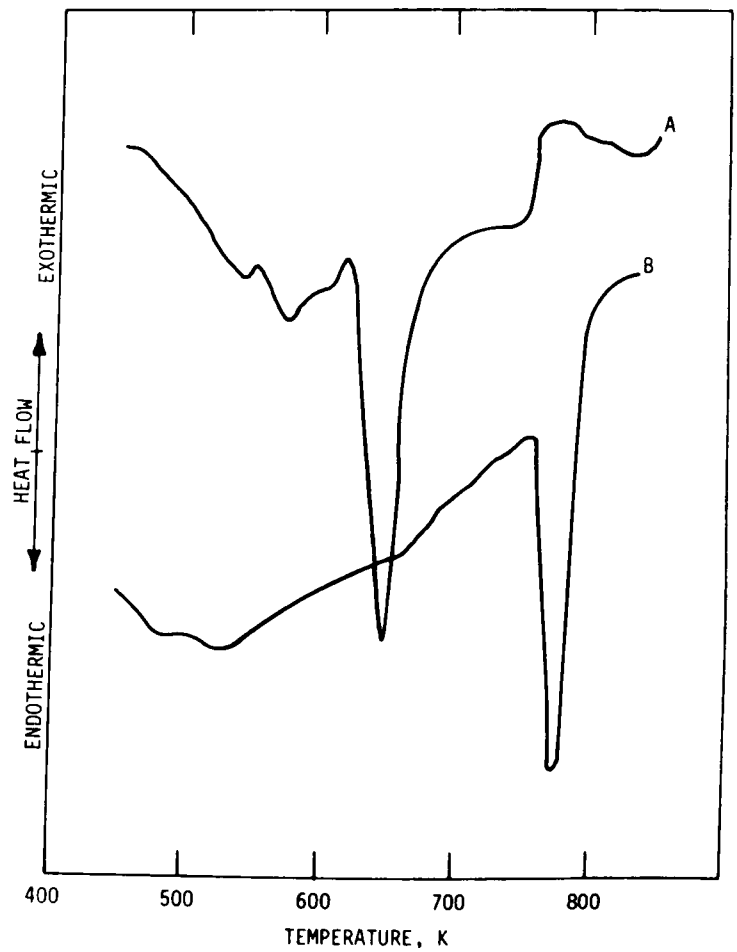

Fig. 1. Thermograms of Electrolyte Powders

The $LiOH-KOH-Al_2O_3$ powder is comminuted in a ball mill and seived to a particle size less than 149 μm (-100 mesh U. S. Standard Seive Series) to ensure the absence of large particles; then, CO_2 is passed over a thin uniform layer of the powder for >12 h without external heating. The powder sample after this first CO_2 treatment is agglomerated but is comminuted relatively easily to -100 mesh. The powder is then heated to 873 K in a CO_2 gas stream for >12 h to ensure complete conversion of the unreacted hydroxides to the carbonate salts and removal of product water. The times of exposure to flowing CO_2 necessary for complete conversion are dependent on the geometry of the experiment, and the minimum exposure times have not yet been determined. Monitoring of the thermograms of samples after various exposure times to CO_2 can be used to indicate the progress of the reaction and thus determine required times for complete conversion under any particular set of experimental conditions.

B. Phase and Structural Stability of $LiAlO_2$

In the last quarterly report (ANL-77-29, pp. 14-15) we presented data showing that, at 973 K, in the presence of molten carbonates ($Li_2CO_3-K_2CO_3$, 0.62/0.38 mole ratio; liquid phase, 55 wt %) β-$LiAlO_2$ underwent a phase transformation to γ-$LiAlO_2$ in less than 100 h in a CO_2 atmosphere. The phase and structural stability of the rodlike β-$LiAlO_2$ particles at 923 K is now being investigated.

Powder samples of β-$LiAlO_2$ mixed with $Li_2CO_3-K_2CO_3$ (55 wt % alkali carbonates; 62 mol % Li_2CO_3-38 mol % K_2CO_3) were heated at 923 K in gas environments simulating molten carbonate fuel cell conditions. Periodically, samples were removed and the $LiAlO_2$ was examined by scanning electron microscopy (SEM) and X-ray diffraction analysis.* After a total of 530 h at 923 K in CO_2/air (the CO_2 was introduced at a low flow rate once the sample was in an oven), the original β-$LiAlO_2$ rod-shaped particles were unaltered in morphology and phase. In identical experiments, except that the gas atmosphere was air or 78% H_2-19% CO_2-3% water, rod-shaped β-$LiAlO_2$ particles have remained unchanged in phase and particle shape for 765 and 750 h; respectively, at 923 K. Presently, these studies are continuing and heating times have been extended past 1000 h; these results will be presented when SEM and X-ray diffraction analyses are completed.

III. CELL TESTING

The primary objective of cell testing at ANL is to understand and control significant properties of the cell components and the changes in these properties during cell lifetimes. The electrolyte and the wet-seal area of the cell housings have received particular attention; characterization of the electrodes and evaluation of the effects of changes in electrode parameters have just begun. Efforts are continuously being made to improve performance

*X-ray diffraction analyses were performed by B. S. Tani of the Analytical Chemistry Laboratory, ANL. The SEM analyses were performed with the assistance of R. Malewicki, also of the Analytical Chemistry Laboratory.

in order to operate cells under conditions most representative of future power plant conditions.

A. Wet-Seal Protection

Beginning this quarter, cell wet seals have been provided with corrosion protection by an aluminizing process as follows: The cell is masked so that only the wet seal area is exposed; then, aluminum metal is flame-sprayed* onto the seal to a depth of 50-75 μm. The housing is then heated to 1275 K for about 30 min *in vacuo* or in an atmosphere of helium so that a diffused layer will be formed between the aluminum and the Type 316 stainless steel base metal. During initial cell operation, the aluminum reacts with the electrolyte and/or the gas atmosphere to form a protective coating of Al_2O_3 and $LiAlO_2$. Wet seals protected in this way have accumulated about 1400 h of use in several cell tests. The seals received no treatment between tests except removal of residual electrolyte with water.

Since cells having protected wet seals were put into use, no measurable leakage of anode gas has occurred. The absence of anode wet-seal leakage is not necessarily due to the wet-seal protection alone, because tile properties (such as rigidity and pore-size distribution) have been changed. Leakage measurements are made by substituting N_2 for the anode gas in order to eliminate uncertainties associated with condensation of H_2O from the fuel gas. The flow rates into and out of the anode chamber are then compared. Any discrepancy of more than 2-3% is attributed to leakage. Cathode leakage is measured in the same way, except that substitution of N_2 is unnecessary.

B. Cell Operation

During this quarter, the CS-series of cells has been operated. Like the earlier KK-series, they are 7-cm-dia, cylindrical cells having porous nickel electrodes (the cathode immediately oxidizes to NiO), Type 316 stainless steel housings and current collectors, and $LiAlO_2$/alkali carbonate tile electrolytes. They differ from the KK-series cells in having protected wet seals and a central support post for the perforated current collector. The support post and other details of construction may be seen in Fig. 2. The heavy housings are reused upon termination of test; all other components are replaced. The electrolytes and cell housings are fabricated at ANL; and the porous electrodes are purchased from Gould Laboratories, Cleveland, Ohio, or from Union Carbide Corporation, Carbon Products Division, Parma, Ohio.

The major variations in Cells CS-1 to -4 are listed in Table 1. Cell CS-1 may be regarded as a baseline cell; its performance is somewhat better than that of any cell we have operated. In Cell CS-2, variations introduced in the anode, cathode, and electrolyte produced decidedly negative results, as may be seen in Fig. 3. These variations are systematically being removed in later cells of the CS-series. The most significant changes are evidently not due to differences in the cathode, or to the amount of anode "bite," i.e., the extent of protrusion above the wet seal, since the use of a cathode identical to that of CS-1 (in Cell CS-3) or an anode with "bite" (Cell CS-4)

---

*Flame-spraying was done by Coating Systems Technology, Inc., North Babylon, N. Y.

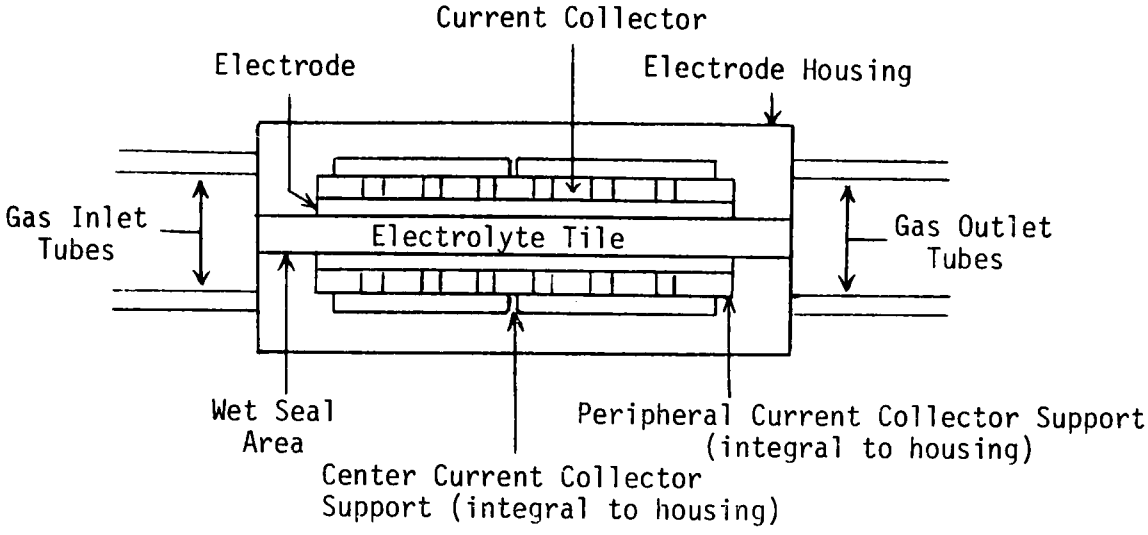

Fig. 2. Schematic of CS-Series Cells

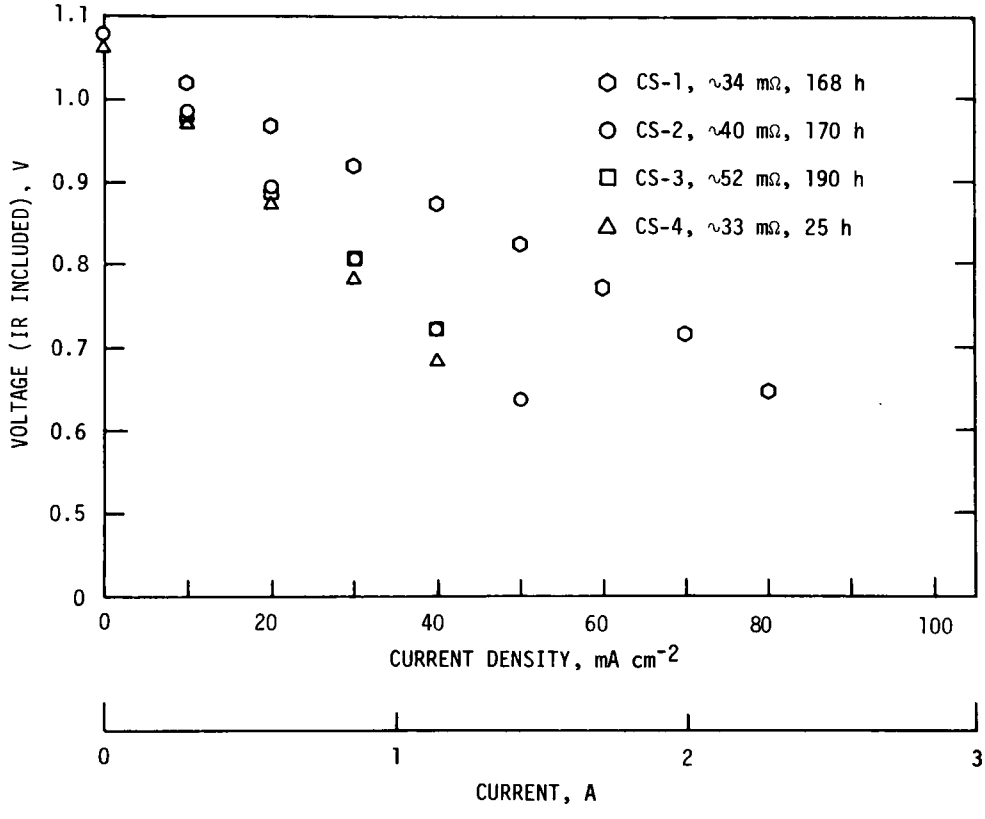

Fig. 3. Comparison of Cell Performance of CS-Series Cells
Temperature: 923 K
Flow rates: 3A (to both electrodes)
Anode gas: 80% H_2, 20% CO_2 saturated at 298 K with H_2O
Cathode gas: 28% CO_2, 14.5% O_2, 57.5% N_2

Table 1. Structural and Performance Characteristics of CS-Series Cells

	CS-1	CS-2	CS-3	CS-4
Anode[a]				
Thickness, cm	0.043	0.033	0.033	0.033
Bite,[b] cm	0.010	0	0	0.015
Cathode				
Electrode Material	Union Carbide 306-24-30B	Union Carbide PMP 1100	Union Carbide 306-24-30B	Union Carbide 306-24-30B
Thickness, cm	0.064	0.030	0.064	0.064
Porosity, %	71.5	73.5	71.5	71.5
Mean pore size, μm	6.6	11.2	6.6	6.6
Bite, cm	0	0.005	0	0.008
Electrolyte Tile				
Thickness, cm	0.19-0.20	0.21-0.22	0.22-0.23	0.22-0.24
Alkali carbonates, wt % (vol %)	55 (68)	55 (61)	55 (61)	55 (61)
$LiAlO_2$ phase	α(maj), γ(min)	β	β	β
$LiAlO_2$ morphology	clumps	rods	rods	rods
Cell Resistance, mΩ	34	41	52	33
Cell Voltage, V, at 40 mA/cm^2 (38% utilization)				
IR included	0.875	0.722	0.723	0.686
IR free	0.913	0.769	0.782	0.723

[a]Anode material, Gould 309-144-3, rolled to thickness shown; originally 0.076 cm thick; porosity 84%, mean pore size 10 μm (quoted by manufacturer).

[b]Protrusion above wet seal on assembly.

did not improve performance. Cells CS-5 and CS-6, now under construction, are intended to be identical to CS-1 in all components except the electrolyte. CS-7 will be an exact reproduction of CS-1. Operation of these cells enables us to determine whether, in fact, the electrolyte is the most significant factor in cell performance, as we suspect.

The major difference in the CS-series cells was the change from an α-$LiAlO_2$ tile containing 68 vol % carbonates (CS-1) to a β-$LiAlO_2$ tile containing 61 vol % carbonates (CS-2 to -4). The initial β-$LiAlO_2$ tiles used in the latter cells appeared to be much softer and more easily deformed than the α-$LiAlO_2$ tiles used in CS-1 and previous cells. This problem may be due to the essentially larger and more uniform size and shape of the β-$LiAlO_2$ particles. As has been pointed out by Maru and Marianowski,[2] a proper balance of pore-size distribution among the anode, cathode, and electrolyte tile is essential to good cell performance. Therefore, a major effort in the future will be directed to optimization of the particle-size distribution in the electrolyte tile, from the standpoint of improving both performance and strength. Smaller particles of $LiAlO_2$ will be admixed to fill the interstices between the rods of β-$LiAlO_2$, thus reducing the pore size and increasing the tile rigidity to a level greater than that of tiles having no rodlike $LiAlO_2$ particles. These tiles are being prepared and will be run in Cells CS-8 and CS-9.

IV. COMPONENT ANALYSIS AND DEVELOPMENT

A. Post-Test Observations

As mentioned in the preceding section, aluminized wet seals have shown excellent corrosion resistance, thus mitigating the main corrosion problem in previous cells. Cathode cell housings and current collectors of the CS-series cells have continued to show a uniform, adherent, hard layer of dark oxide. Anode housings and current collectors have shown apparently random patches of scale-type corrosion products, especially in the perforations of the Type 316 stainless steel current-collector plates.

We have continued to observe diffused layers of NiO up to 0.2 mm thick on the cathode side of the tile. Cathodes are normally strongly adherent to the tile; anodes are strongly adherent only occasionally. Even when the anode is embedded in the tile, no evidence is ever seen of a diffused Ni or NiO layer on the anode side of the tile.

B. Characterization of Porous Nickel Electrodes

The surface area and porosity are physical parameters which play an important role in the performance of porous electrodes in molten carbonate fuel cells. The porosity and pore-size distribution of the porous electrodes and the $LiAlO_2$ structure (tile) must be balanced so that some of the electrolyte moves from the $LiAlO_2$ matrix to the porous electrode but does not flood the electrode or leave open porosity in the tile.

Information on the porosity and surface area of the porous electrodes in our molten carbonate fuel cells was obtained by means of mercury porosimeter

measurements.* This information is expected to aid in determining the electrolyte distribution between the porous electrode and the $LiAlO_2$ matrix; a knowledge of this distribution is necessary to optimize cell performance.

The porous electrode surface area was determined from standard porosimeter pressure-volume curves by the method outlined by Rootare and Prenzlow.[3] Briefly, the reversible work required to immerse a mass of powder, of area, da, in mercury is considered to be equal to the work supplied when an external pressure, P, forces a volume of mercury, dV, into the pores of the powder. Hence,

$$\gamma_L \cos \Theta \, da = -P \, dV \tag{1}$$

where cos Θ is the contact angle between mercury and the solid surface (Θ is taken to be 130°) and γ_L is the surface free energy of liquid mercury *in vacuo* (4.8×10^{-5} J/cm^2). If the porosimetry measurements are made at 298 K (25°C), the specific surface area, A(m^2/g), is given by

$$A = \frac{3.268 \times 10^{-3}}{m} \int_0^{V_{max}} P \, dV \tag{2}$$

where m is the mass (g) of powder, P is the pressure (kPa), and V is the volume (cm^3).

Figure 4 shows the mercury porosimetry data obtained on four porous nickel electrode materials. For a given value of applied pressure, the pore diameter, d, can be calculated from the capillarity equation of Washburn,[4]

$$d = \frac{-4\gamma_L \cos \Theta}{P} \tag{3}$$

As the pore diameter becomes smaller, a greater pressure is required to cause the mercury to enter the pore. The pore diameter corresponding to a given pressure is shown on the right-hand side of Fig. 4.

The porosities and specific surface areas of the nickel electrodes determined from the data in Fig. 4 are presented in Table 2. (The masses of electrodes used in calculating specific surface areas did not include the masses of the metal screens used in the electrode structure.) For the range of specific surface areas listed in Table 2, the average particle size of the nickel is 3-4 μm, assuming that the particles are spherical.

The pore size distribution of the electrodes can be obtained by analysis of the data in Fig. 4. The slope of the curve for P *vs.* V, after substitution of Eq. 3, yields

$$\frac{dV}{dP} = - \frac{(dV/dr) r^2}{2\gamma \cos \Theta} \tag{4}$$

---

*Measurements were made through the courtesy of the Institute of Gas Technology, Chicago, Ill.

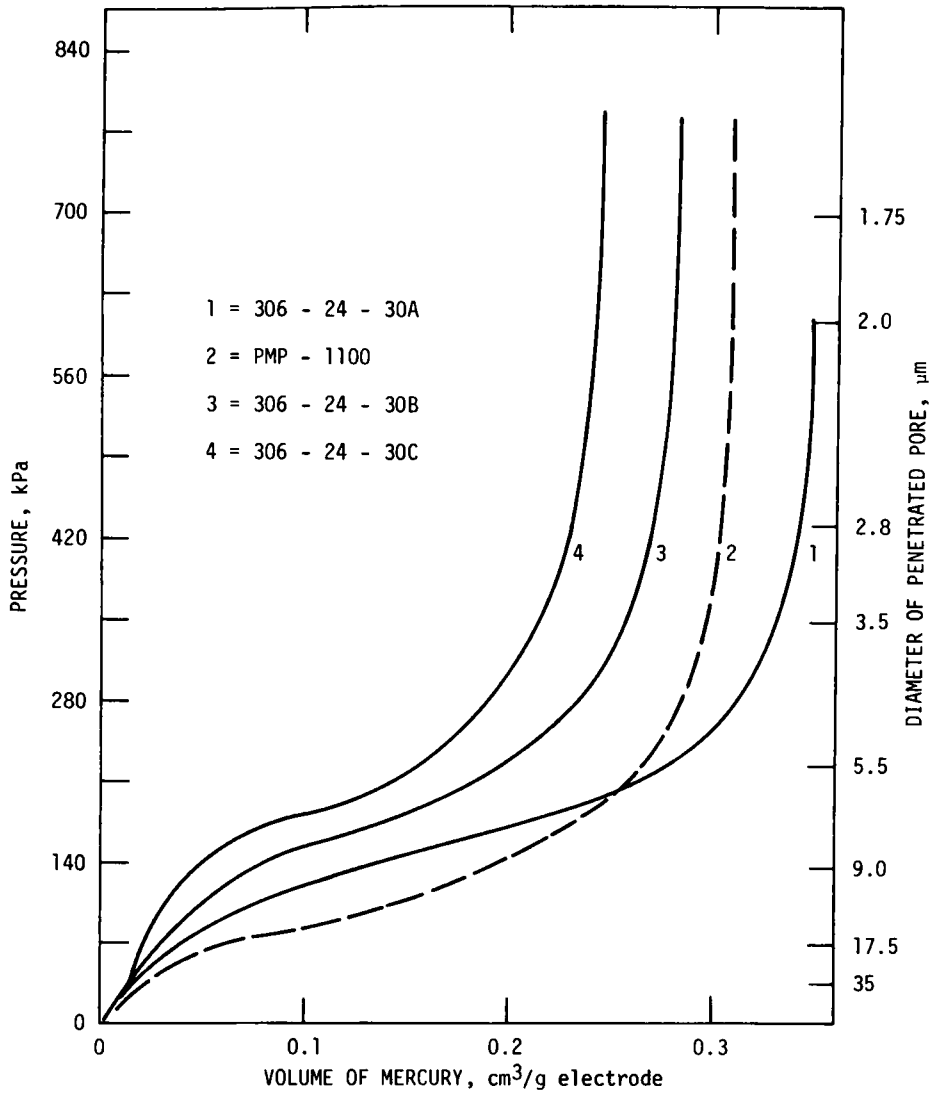

Fig. 4. Mercury Penetration of Nickel Electrodes

Table 2. Porosities and Surface Areas of Porous Nickel Electrodes

Electrode Material Designation	Porosity, %	Mean Pore Size, µm	Specific Surface Area, m^2/g	Fuel Cell Application
306-24-30A	75.7	7.7	0.25	Cathode JS-1, KK-1 to KK-8
306-24-30B	71.5	6.6	0.22	Cathode CS-1, CS-3, CS-4
306-24-30C	68.5	6.1	0.21	Anode JS-1, KK-1 to KK-7
PMP-1100	73.5	11.2	0.17	Cathode CS-2

where r is the pore radius. The volume, V, of pores of radii between r and r + dr is dV, which is related to r by some distribution function, D(r):

$$D(r) = dV/dr \tag{5}$$

Therefore, the distribution function is related to the slope, dV/dP, by the equation

$$D(r) = (P/r)\ dV/dP \tag{6}$$

and the resulting distribution curve [D(r) *vs.* r] gives the volume of pores which have a given radius. Analysis of the data in Fig. 4 by this technique yields the distribution curves plotted in Fig. 5, where it is evident that the electrode material PMP-1100 has a wider distribution of pore sizes than the other electrode materials.

Extrapolation of the data in Figs. 4 and 5 to interpret fuel cell performance is tenuous, since the physical characterization of the electrolyte tiles is incomplete. However, some observations seem worthwhile. Consider fuel cells CS-2 and CS-3, which both had anodes of the same material (Gould 309-144-3 electrodes compressed to 0.033 cm) and similar electrolytes (β-$LiAlO_2$ rod-shaped particles mixed with 55 wt % Li_2CO_3-K_2CO_3). The cathode materials of Cells CS-2 and CS-3 were PMP-1100 and 306-24-30B, respectively; these materials had similar porosities but different mean pore sizes and pore-size

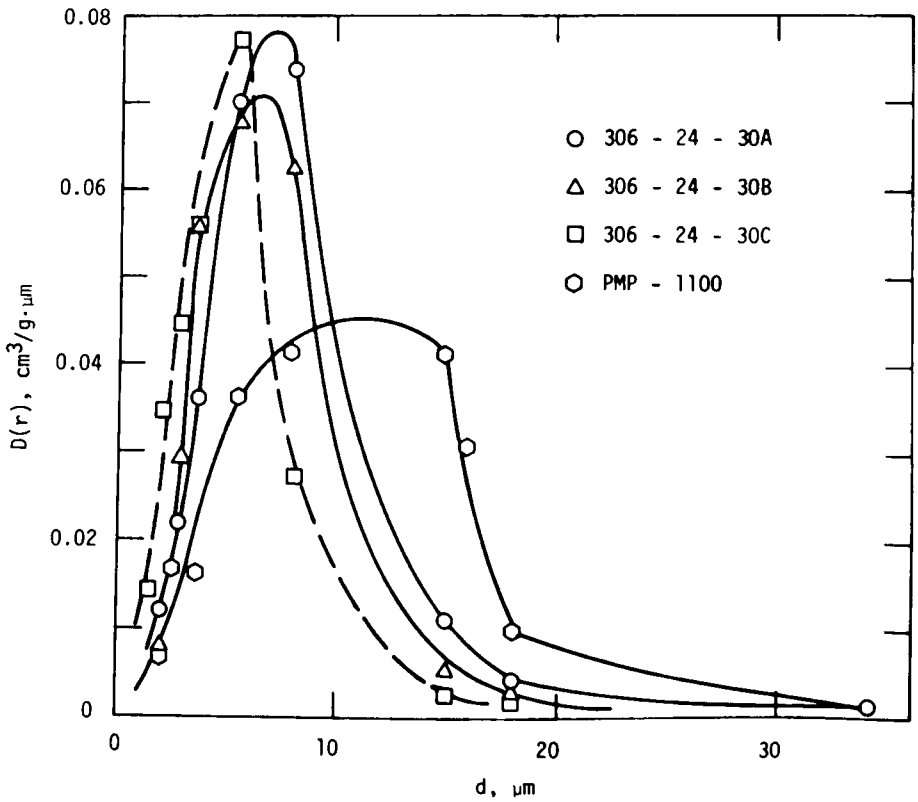

Fig. 5. Distribution of Pores in Nickel Electrodes

distributions (see Table 2 and Fig. 5). However, the similarity of the fuel cell performances (see Fig. 3) suggests that the differences in the pore size distributions and mean pore sizes for the cathodes in these two fuel cells had very little influence on fuel cell performance. Possible explanations for the similar performances include the following: (1) the anode performance is the limiting factor or (2) the cathodes of both cells were either electrolyte-starved or electrolyte-flooded.

Mercury porosimetry measurements of porous electrodes will be continued to obtain porosity and surface-area data. This information, coupled with a better understanding of the $LiAlO_2$ structure in the electrolyte tiles, should provide a better knowledge of the factors that affect fuel cell performance.

C. Tile Diagnostics

The static creep apparatus described in our previous quarterly report (ANL-77-29, p. 39) has been rebuilt, making extensive use of quartz components (see Fig. 6). It now performs very well. Blank runs in which the apparatus

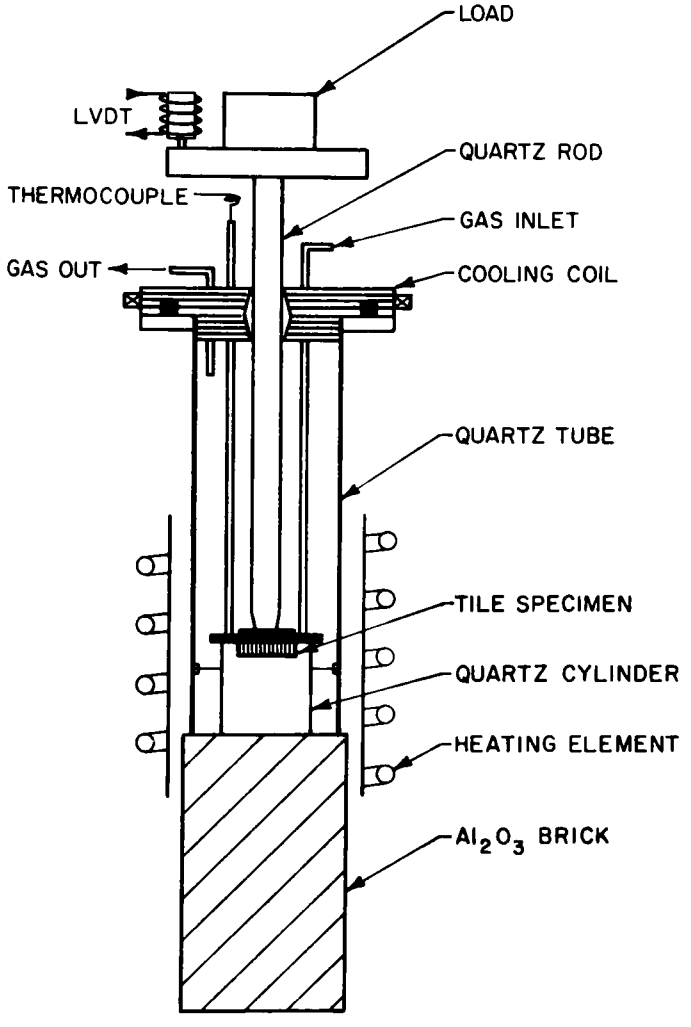

Fig. 6.

Modified Static Creep Apparatus (LVDT = Linear Voltage Differential Transducer)

was cycled between room temperature and 973 K showed a zero-point displacement in the linear voltage differential transducer corresponding to less than 18 μm, an improvement of more than four-hundredfold. Thermal expansion measurements on Type 316 stainless steel specimens under a load of 100 kPa (14 psi) between ambient temperature and 973 K gave excellent agreement with the literature value[5] for the coefficient of expansion, α_t, namely, 19.3 × 10^{-6}/K *vs.* the literature value of 20 × 10^{-6}/K.

Initial experiments on the static creep behavior of titles are being conducted on tiles containing 34, 39, 44, and 49 vol % α- or β-$LiAlO_2$ in alkali carbonate (62 mol % Li_2CO_3, 38 mol % K_2CO_3). Table 3 gives the results of measurements of thermal expansion and creep rate on three tile specimens in CO_2 or H_2 + CO_2. Figure 7 shows the thermal behavior of these specimens.

Table 3. Thermal Measurements on Electrolyte Tiles

Tile No. (Sample No.)	Tile Composition[a]	Specimen Thickness, mm	Environment	Load, kPa	10^6 α_t,[b] K^{-1}	10^6 × Creep Rate at 923 K, h^{-1}
D13AF (1)	α-$LiAlO_2$, 45 wt % (32 vol %)	6.7	CO_2	97	12.5	-945[c]
D84-26-2 (3)	β-$LiAlO_2$, 54 wt % (48 vol %)	6.8	CO_2	105	10.5	-36[d]
D84-26-2 (2)	β-$LiAlO_2$, 54 wt % (48 vol %)	6.8	80% H_2-20% CO_2	93	9.0	-30[e]

[a]Remainder, 62 mol % Li_2CO_3-38 mol % K_2CO_3.

[b]Between room temperature and 753 K.

[c]Between 873 and 973 K; measured over a period of 50 h.

[d]Measured over a period of 194 h.

[e]Measured over a period of 162 h.

A common feature in all of these curves is that the expansion of tile is almost linear between room temperature and melting point (∿753 K) of the carbonates in the specimen. The α_t values for the tiles containing 45 to 54 wt % of $LiAlO_2$ are in the range from 9 to 12.5 × 10^{-6} K^{-1}. During these measurements, the compression load on the specimens was kept constant at about 100 kPa (∿14 psi). Further data are needed before a relationship among the observed α_t, carbonate content, and the allotropic form of $LiAlO_2$ can be predicted.

The second common feature among these measurements is that the tiles contract at the melting point of the carbonates, as expected. Larger contractions were also expected of tiles containing larger percentages of carbonates. In Fig. 7, Sample 1 (68 vol % carbonates) produced a much larger contraction

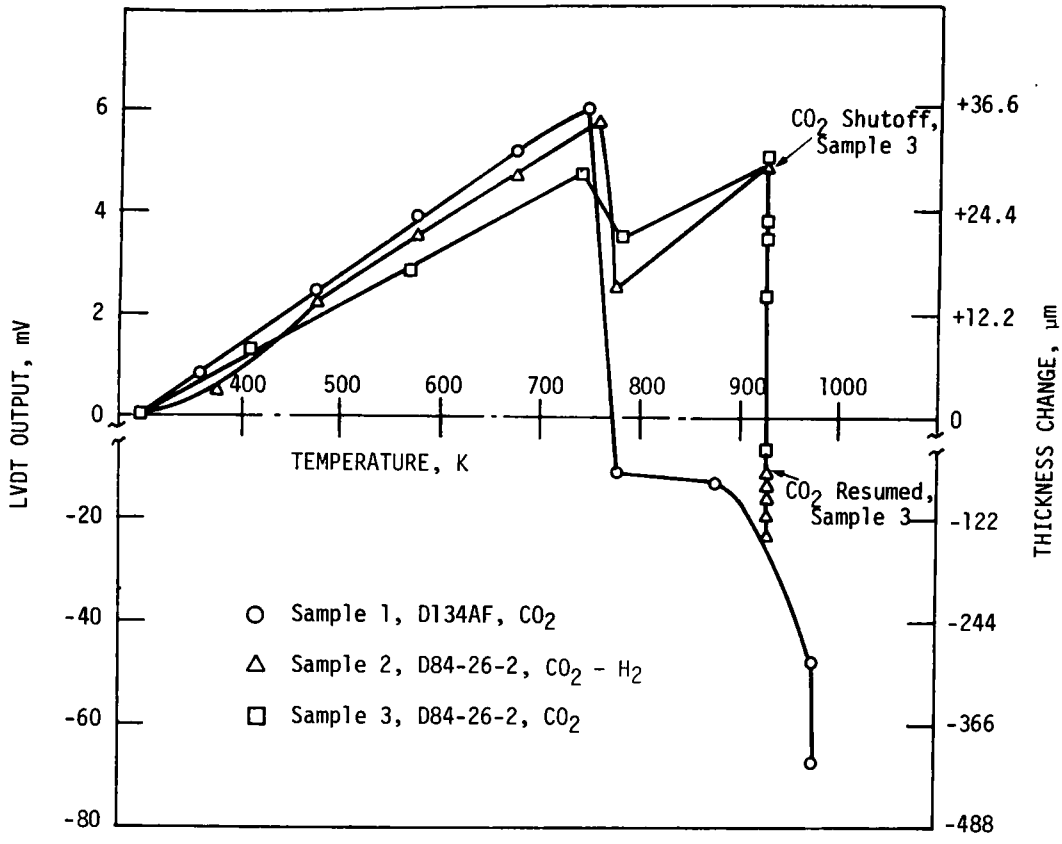

Fig. 7. Thermal Expansion and Creep-Rate Measurements on Electrolyte Tiles (Time periods for creep-rate measurements: Sample 1, 50 h; Sample 2, 162 h; Sample 3, 192 h)

than Samples 2 and 3 (containing 52 vol % carbonates). The creep rate of Sample 1, measured nonisothermally between 873 and 973 K, exceeds that measured at 923 K on specimens 2 and 3 by a factor of about thirty. This magnitude of difference is unexpected, even though the difference in carbonate content was 16 vol %.

An important point is that during these measurements the atmosphere surrounding the sample must contain CO_2. Sample 3 experienced an accidental cessation of gas flow, and apparently decarbonated rapidly, with a concomitant, sudden shrinkage of about 100 µm. Resumption of gas flow reduced the shrinkage rate to normal creep-rate levels.

Further work in this area will consist of measuring the thermal behavior of tiles of various compositions in cathodic as well as anodic gaseous environments, and correlating the results with specific surface area measurements, electron microscopy of the $LiAlO_2$, and tile behavior in cells.

REFERENCES

1. *JANAF Thermochemical Tables*, 2nd Ed., NSRDS-NBS37 (1971).

2. H. C. Maru and L. G. Marianowski, Abstract No. 31, Fall Meeting of the Electrochemical Society, Las Vegas, Nevada, Oct. 17-22, 1976.

3. H. M. Rootare and C. F. Prenzlow, J. Phys. Chem. *71*, 2733 (1967).

4. E. W. Washburn, Proc. Nat. Acad. Sci. *7*, 115 (1921).

5. *Metals Handbook*, Vol. 1, 8th Ed., American Society for Metals (1961).

Distribution for ANL-77-56

Internal:

E. G. Pewitt
J. P. Ackerman (25)
E. M. Bohn
L. Burris
F. A. Cafasso
L. Cuba
J. Harmon
R. O. Ivins
G. M. Kesser
K. Kinoshita
A. Melton
P. A. Nelson (20)
J. W. Sim
R. K. Steunenberg
R. Swaroop
A. D. Tevebaugh
D. S. Webster
A. B. Krisciunas
ANL Contract Copy
ANL Libraries (5)
TIS Files (6)

External:

ERDA-TIC, for distribution per UC-93 (171)
Manager, Chicago Operations Office
Chief, Chicago Patent Group
President, Argonne Universities Association
Chemical Engineering Division Review Committee:
  R. C. Axtmann, Princeton U.
  R. E. Balzhiser, Electric Power Research Inst.
  J. T. Banchero, U. Notre Dame
  D. L. Douglas, Gould Inc.
  P. W. Gilles, U. Kansas
  R. I. Newman, Allied Chemical Corp.
  G. M. Rosenblatt, Pennsylvania State U.
T. R. Beck, Electrochemical Technology Corp., Seattle
K. Blurton, Inst. of Gas Technology, Chicago
A. Borucka, Borucka Research Co., Livingston, NJ
D. Chatterji, General Electric Co., Schenectady
G. Ciprios, Exxon Research and Engineering Co., Linden, NJ
L. M. Ferris, Oak Ridge National Lab.
A. P. Fickett, Electric Power Research Inst.
J. Huff, U. S. Army Mobility Equipment R&D Center
J. M. King, United Technology Corp.
A. R. Landgrebe, Div. of Energy Storage Systems, USERDA
L. R. Lawrence, Div. of Conservation Research and Technology, USERDA (3)
J. J. Rasmussen, Montana Energy and MHD Research Inst.
R. Roberts, The Mitre Corp.
E. Yeager, Case Western Reserve U.